Nuclear Engineering and Technology 52 (2020) 1907–1916

Contents lists available at ScienceDirect

Nuclear Engineering and Technology

journal homepage: www.elsevier.com/locate/net

Original Article

Validation of nuclide depletion capabilities in Monte Carlo code MCS

Bamidele Ebiwonjumi, Hyunsuk Lee, Wonkyeong Kim, Deokjung Lee*

Department of Nuclear Engineering, Ulsan National Institute of Science and Technology, 50 UNIST-gil, Ulsan, 44919, Republic of Korea

ARTICLE INFO

Article history:
Received 14 March 2019
Received in revised form
9 January 2020
Accepted 25 February 2020
Available online 29 February 2020

Keywords:
MCS
Depletion
Spent nuclear fuel
Validation
Isotopic inventory

ABSTRACT

In this work, the depletion capability implemented in Monte Carlo code MCS is investigated to predict the isotopic compositions of spent nuclear fuel (SNF). By comparison of MCS calculation results to post irradiation examination (PIE) data obtained from one pressurized water reactor (PWR), the validation of this capability is conducted. The depletion analysis is performed with the ENDF/B-VII.1 library and a fuel assembly model. The transmutation equation is solved by the Chebyshev Rational Approximation Method (CRAM) with a depletion chain of 3820 isotopes. 18 actinides and 19 fission products are analyzed in 14 SNF samples. The effect of statistical uncertainties on the calculated number densities is discussed. On average, most of the actinides and fission products analyzed are predicted within ±6% of the experiment. MCS depletion results are also compared to other depletion codes based on publicly reported information in literature. The code-to-code analysis shows comparable accuracy. Overall, it is demonstrated that the depletion capability in MCS can be reliably applied in the prediction of SNF isotopic inventory.

1. Introduction

The application of Monte Carlo (MC) methods in the solution of reactor physics problem is becoming more attractive due to advances in computational resources and demand for high-fidelity physics solution. MC methods are advantageous in that they allow for explicit geometry modeling and usage of continuous energy cross-sections. The major drawback in the widespread adoption of MC methods in the reactor physics community is the large amount of computing time and memory required in MC simulations. However, with the possibility of parallel computation, MC methods may soon be used practically in routine simulations.

Over the years, MC neutron transport coupled to nuclide depletion has been performed by linking an independent MC transport code such as MCNPX or Shift to external depletion codes such as CINDER [1] or ORIGEN [2]. Nowadays, there are many Monte Carlo codes which couple the transport simulation and the prediction of actinide/fission product buildup internally. Codes using this type of built-in depletion system include McCARD [3], SERPENT [4], MVP-BURN [5], and RMC [6].

In this paper, we present the validation of the nuclide depletion capability implemented into the MC code MCS. The purpose of this validation is to quantify and analyze the bias and uncertainties associated with the predicted isotopic compositions. The bias is the (C/E − 1) ratio in percent where *C* and *E* are the calculated result and experimental data, respectively. The uncertainty is the standard deviation of the (C/E − 1) ratio. Uncertainties due to covariance of nuclear data in a depletion calculation are not presented in this manuscript. The validation work presented here is important for use in spent nuclear fuel (SNF) applications such as criticality safety, burnup credit and cask dose rate analysis. This is also important because MCS is developed to become a reference code for other codes in a verification and validation (V&V) exercise. MCS is a three-dimensional (3D) continuous-energy neutron-photon transport MC code under development at the Ulsan National Institute of Science and Technology (UNIST) since 2013. MCS is developed for analysis of large scale nuclear reactors with fuel depletion, thermal-hydraulic and fuel performance feedback [7]. MCS features a built-in depletion solver to explicitly track thousands of nuclides in its burnup chain.

Measurement programs have been established in the past 50 years to obtain assay data of SNF and are now well accepted internationally as benchmarks. Especially, efforts have been devoted to set up a database of isotopic assay data grouping together the information from those internationally-established programs. Such a database is the Spent Fuel Isotopic Composition Database (SFCOMPO), distributed by the Nuclear Energy Agency

* Corresponding author.
E-mail addresses: ebiwonjumi@unist.ac.kr (B. Ebiwonjumi), hyunsuklee@unist.ac.kr (H. Lee), poryor@unist.ac.kr (W. Kim), deokjung@unist.ac.kr (D. Lee).

https://doi.org/10.1016/j.net.2020.02.017

(NEA) of the Organization for Economic Co-operation and Development (OECD) since 2002 [8,9].

SNF assay data obtained from SFCOMPO database is selected as benchmark to validate the depletion capability of MCS in this work. In addition, we compare the results of MCS depletion to the results of other depletion code systems obtained from reports published in the literature. The other codes may feature different burnup chain model, cross section/decay/fission yield/isomeric branching ratio data, power to flux normalization, power history decomposition and modeling. Nevertheless, they have been employed because they have been benchmarked and therefore are suitable for comparison in order to verify the results of MCS. Except otherwise stated, all the results presented in this work are obtained with the ENDF/B-VII.1 cross section and decay/fission yield data.

The plan of this work is as follows. First, we describe the measurement data used for the depletion validation. Second, the computational methods applied in MCS are discussed, and the computational model used to analyze the benchmark is presented. Third, the bias and uncertainties associated with the predicted isotopic compositions in MCS are quantified and analyzed. Then the effect of statistical uncertainties during the depletion calculation is also discussed. Fourth, the results of MCS depletion are compared to other depletion codes. Fifth, the conclusions are summarized.

2. Measurement data of spent nuclear fuel compositions

Post irradiation examination (PIE) data are used for the validation of MCS. The data set contain benchmark SNF isotopic data measured from the destructive analysis of fuel samples cut from fuel rods irradiated in one PWR operated Japan. The experimental methods applied include α-, and γ-spectrometry, isotope dilution mass spectrometry (IDMS), thermal ionization mass spectrometry (TIMS), inductively coupled plasma mass spectrometry (ICPMS) and luminescent analysis (LA). The PIEs were carried out by Japan Atomic Energy Research Institute (JAERI), now Japan Atomic Energy Agency in Japan, for the measurement of the isotopic content of the SNF samples from the Takahama-3 PWR. The JAERI measurements are summarized in the SFCOMPO database and the benchmark is presented in detail in the reference [10]. The characteristics of the measured fuel are summarized in Tables 1 and 2. Table 1 contains the reactor name, the fuel enrichment, number of fuel samples, fuel sample burnup, the number of irradiation cycles, the IDs of the fuel rods from which the measured samples were taken and the fuel type. The sample identifier, the assembly from which the samples were taken, and the position of the sample from the bottom of the fuel rod active length, and the sample burnup are presented in Table 2. All the measured fuel rods come from assemblies which include gadolinium fuel rods. All the assembly designs considered have 17 x 17 pins. The measured fuel samples were obtained from fuel rods having initial enrichments from 2.6 to 4.1 wt% ^{235}U and burnups from 14 to 47 GWd/t. The locations of the fuel rods from which the measured samples were obtained are shown in Fig. 1. For the Takahama-3 assembly, the SF95 rod is the fuel rod at the corner of the assembly; SF97 is the fuel rod in the middle of the assembly side and SF96 rod is located adjacent to a guide tube. A total of ten uranium dioxide (UO_2) and four gadolinium (UO_2-Gd_2O_3) SNF samples are analyzed for actinides and fission products of interest to burnup credit, criticality safety, radioactive waste management and radiation safety applications.

3. Description of the Monte Carlo code MCS

3.1. Computational methods

MCS is a 3D continuous energy radiation transport Monte Carlo code under development at UNIST. MCS is designed for the criticality analysis of large scale nuclear reactors with fuel depletion and thermal-hydraulics feedback. MCS has been applied in criticality safety analysis of spent fuel pool and storage cask, radiation shielding, and cask dose rate analysis. MCS solves criticality/eigenvalue, fixed-source, and multi-physics problems. MCS neutron transport kernel has been validated against ~300 critical cases of the International Criticality Safety Benchmark Experimental Problem (ICSBEP) [11], BEAVRS benchmark [12], VENUS-2 and Hoogenboom Martin benchmark [13,14]. MCS photon fixed-source runs have been verified against reference Monte Carlo codes for shielding problems [15]. MCS has been coupled with the subchannel code CTF [16], fuel performance code FRAPCON [17] and thermal-fluid code GAMMA+ [18] for high fidelity multi-physics applications. Extensive V&V of MCS in the solution of large scale commercial light water reactor whole core depletion and multi-cycle operation is ongoing [19–23].

MCS features a variety of temperature dependent on-the-fly cross section processing capabilities. In the resolved resonance range, the multipole representation is used to calculate Doppler broadened cross-sections [24]. The probability table (PT) method is used in the unresolved resonance range to account for self-shielding effects and to generate self-shielded cross section. PT is used in this work [25]. In the thermal range, interpolation function is used to generate broadened thermal scattering data [26]. In this study, S(α, β) of ^{1}H in light water is used. The free-gas treatment is used for all the nuclides including ^{1}H. For ^{1}H, both S(α, β) and the free-gas treatment are selectively used depending on the incident neutron energy. In the thermal energy range, S(α, β) is used. And the free-gas treatment is used for all energy range except the thermal energy range. Doppler Broadening Rejection Correction (DBRC) is used to consider resonance scattering due to thermal motion of heavy target nuclides.

MCS tallies the one-group neutron flux and reaction rates during the transport simulation, for use in the depletion calculation. The depletion solver takes advantage of the parallel calculation capabilities present in MCS. Burnup calculations in MCS employs a depletion chain of 3820 nuclides (all the nuclides in the ENDF decay library) and solves the transmutation equation by the Chebyshev Rational Approximation Method (CRAM) [27]. All the decay modes stated in the ENDF/B-VII.1 decay library is accounted for in detail. 6 neutron-induced reaction types are considered: (n, γ), (n, $2n$), (n, $3n$), (n, α), (n, p) and (n, *fission*), where the fission reaction rates are tallied in three-group. On-the-fly energy released per fission is used to obtain kappa values. Full and semi predictor-corrector depletion

Table 1
Characteristics of PWR spent fuel rods for the PIE[a].

Reactor[b]	Enrichment (wt.%^{235}U)	No. of samples	Burnup (GWd/t)	No. of cycles	Fuel rod ID	Fuel
Takahama-3	4.11	5	14.3–30.4	2	SF95	UO_2
	4.11	5	30.7–47.3	3	SF97	UO_2
	2.63	4	16.4–28.9	2	SF96	UO_2-Gd_2O_3

[a] The measurement facility is JAERI.
[b] Fuel assembly design is 17 x 17.

Table 2
Main parameters of the measured spent fuel samples.

Reactor	Assembly ID	Sample ID	Axial location[a] (mm)	Sample burnup (GWd/t)
Takahama-3	NT3G23	SF95-1	3606	14.30
		SF95-2	3446	24.35
		SF95-3	2926	35.42
		SF95-4	1646	36.69
		SF95-5	246	30.40
		SF96-2	3471	16.44
		SF96-3	2951	28.20
		SF96-4	1671	28.91
		SF96-5	271	24.19
	NT3G24	SF97-2	3457	30.73
		SF97-3	3180	42.16
		SF97-4	1968	47.03
		SF97-5	881	47.25
		SF97-6	251	40.79

[a] Distance measured from bottom of fuel active length.

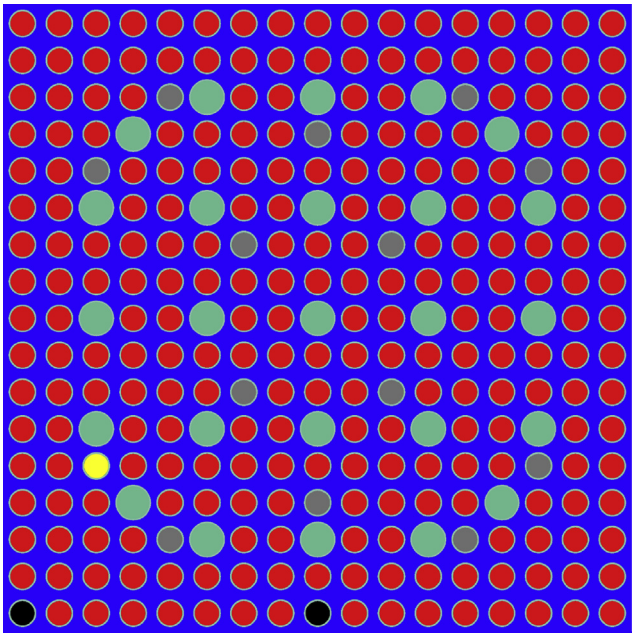

Fig. 1. Fuel assembly geometry showing locations of fuel rods containing the measured samples.
Legend: red (UO_2), gray (UO_2-Gd_2O_3), black (measured UO_2), yellow (measured UO_2-Gd_2O_3), blue (moderator), green (guide tube). (For interpretation of the references to colour in this figure legend, the reader is referred to the Web version of this article.)

schemes are implemented in MCS to reduce time-discretization error during burnup calculation. For the depletion of gadolinium fuel, a quadratic depletion method is used [28]. Details of the computational methods in MCS can be found in the reference [7]. The data used in MCS transport and depletion calculations in this work is based on ENDF/B-VII.1 cross section and decay/fission yield. However, ENDF/B-VII.0 data is used in Section 4.2 to investigate some discrepancies in the (C/E − 1) and in Section 4.5 to perform code-to-code comparison.

3.2. Computational models

The burnup calculation model used to interpret the experimental benchmark is a two-dimensional (2D) representation of the fuel assembly from which the fuel rods and samples were obtained. Reflective boundary conditions have been adopted in the depletion calculations and detailed irradiation histories and fuel assembly specifications are modelled. In a typical fuel assembly depletion calculation, the assembly power is required and given as an input parameter. However, for the benchmarks analyzed in this study, the assembly power is not given. What is given is the power history of the fuel samples *i.e.*, pin power. Because of this, MCS normalizes the reaction rate with the power tallied in the measured fuel rod in order to obtain the normalization factor which will be used in the depletion calculation. The pellet region of the gadolinium-bearing fuel rods is divided into ten equal-volume rings. All the fuel rods in each assembly considered are depleted independently. The geometry of the fuel assemblies is modelled in full. ¼ or 1/8 symmetry condition is not applied in the calculations and the reaction rates are tallied in each of the fuel pins. There is no information on neighboring assemblies, thus, they were not included in the simulations, *i.e.*, single assembly model is used.

The reactor operation data, namely, the power and boron concentration history, fuel pin specifications, and fuel temperature for each of the fuel samples were obtained from the benchmark documentations [9,10]. For all the fuel samples, the axial variation in the neutron spectrum is considered through the different power history and the axial variation in the temperature of the moderator. The local neutron spectrum is largely influenced by the moderator density because of its significant impact on the neutron thermalization. For cases in which the moderator temperature or density at the sample axial location is not available, it was determined based on 2 assumptions: 1) the increase in moderator temperature is proportional to the integrated power from the end of the fuel active length to the sample location 2) the axial power distribution is a cosine function of the fuel active height. With the moderator temperature determined, the moderator density was estimated from temperature versus pressure tables.

For the transport calculations, 50 inactive and 200 active cycles are simulated with 100,000 neutron histories. Five million neutrons are used to converge the fission source distribution and 20 million neutrons are transported during the active cycles before each depletion step. Large number of neutron histories are employed for the 2D problems to reduce the statistical uncertainties. The maximum size of the burnup steps during the depletion calculation is ~2.5 MWd/Kg. The number of burnup steps used to deplete all the fuel samples varies for instance from 51 steps for a final burnup of 14 MWd/kg to 70 steps for a final burnup of 47 MWd/kg.

The fuel sample burnup in the benchmark documentation were determined by the ^{148}Nd method [29], a widely used burnup indicator, because of the high accuracy of ^{148}Nd measurement by isotopic dilution mass spectrometry. The burnup determined by the ^{148}Nd method has an uncertainty of about 3%. The fuel sample

burnups given in the benchmark documentation were reproduced by MCS. Thus, in this study, the fuel sample burnups were not adjusted.

4. Results and discussion

The calculation-to-experiment ratio (C/E), where C is the calculated value and E is the experimental value, is used to compare the calculated and the measured isotopic data from the benchmark. The measurement uncertainties (at one standard deviation) of nuclides measured in the samples are presented in Table 3. These uncertainties account for only the accuracy/precision of the measurement instruments and methods. These uncertainties do not include uncertainties in fuel sample dissolution, uncertainties in chemical separation of elements before isotopic contents are measured by spectrometric techniques, and uncertainties in isotopic dilution. These do not represent the uncertainties at all the steps during the measurement and from all sources of uncertainty *i.e.*, not total.

For each of the nuclide, the (C/E) value is provided in detail against the sample burnup in the appendix (Tables A, B and C) to highlight potential burnup or sample axial position dependence of the (C/E) values, detect trends and identify potential outlier measurements. Potential outlier measurement might be due to difficulty in measuring the very small number densities, such as isotopes of americium and curium. It could also be due to the small accuracy of the measurement method. As the (C/E) values in the appendix show, no obvious trend with burnup is observed for the uranium isotopes. The minor actinides, *i.e.*, ^{237}Np, ^{241}Am and ^{242,243,245,246}Cm display a large spread in their (C/E) values, and they have large (C/E) standard deviation greater than 10%. The reason for this large standard deviation is explained in Section 4.3. Among the major actinides, ^{234}U shows the largest spread in (C/E) values. A noticeable trend in nuclide (C/E) values due to sample burnup/axial location is observed and concerns the SF95-1 sample of Takahama-3. This sample is obtained from an axial location close to the top of the SF95 rod and has a low burnup of 14 GWd/tU. Compared to the other Takahama-3 results, SF95-1 shows a different (C/E) value in ^{239,241,242}Pu (overestimation), and ^{243}Am (large overestimation). This sample is irradiated by a neutron spectrum which is different from the rest of the fuel. Overall, no clear outlier (C/E) value is observed and the authors trust all the measurements with an equal confidence level.

Based on the fuel assembly model developed in the previous section, the (C/E) comparison is summarized in Tables 4 and 5 for measured actinides and fission products respectively. The nuclides shown in these tables are important to radioactive waste management, radiation safety, decay heat, radiation source terms and burnup credit according to OECD/NEA [30]. Due to the lack of a complete set of measurement uncertainty noted at the beginning of this section, the average (C/E) values shown in Tables 4 and 5, are not weighted with the available experimental uncertainties. They are the simple averages of the (C/E) values from each of the fuel samples in which the nuclide was measured. It should be noted that an average (C/E) "forgets" about the burnup dependence of the (C/E) values and places an equal confidence level on all the measurements (in the absence of potential outliers). The value σ shown in Tables 4 and 5 for each nuclide is the sample standard deviation of the (C/E) values (see the footnotes of Table 4).

As shown in Tables 4 and 5, for most of the actinides and fission products, MCS depletion results obtained with ENDF/B-VII.1 lie within 6% of the measured values. Overall agreement with experiment is good. We start by reviewing the individual (C/E) ratios based on the ENDF/B-VII.1 results, for nuclides of interest to source term analysis and burnup credit applications. Then we compare ENDF/B-VII.1 and ENDF/B-VII.0 results for the SF97-4 sample. We

Table 3
Nuclide measurement uncertainties for the samples analyzed in this work (1-sigma, %).

Sample	SF95*/SF96*SF97*
^{234}U	1.0
^{235}U	0.1
^{236}U	2.0
^{238}U	0.1
^{237}Np	10.0
^{238}Pu	0.5
^{239}Pu	0.3
^{240}Pu	0.3
^{241}Pu	0.3
^{242}Pu	0.3
^{241}Am	2.0
^{243}Am	0.5
^{242}Cm	10.0
^{243}Cm	2.0
^{244}Cm	2.0
^{245}Cm	2.0
^{246}Cm	0.5
^{247}Cm	10.0
^{106}Ru	5.0
^{134}Cs	3.0
^{137}Cs	3.0
^{144}Ce	10.0
^{142}Nd	0.1
^{143}Nd	0.1
^{144}Nd	0.1
^{145}Nd	0.1
^{146}Nd	0.1
^{148}Nd	0.1
^{150}Nd	0.1
^{154}Eu	3.0
^{147}Sm	0.1
^{148}Sm	0.1
^{149}Sm	0.1
^{150}Sm	0.1
^{151}Sm	0.1
^{152}Sm	0.1
^{154}Sm	0.1

Table 4
C/E results for actinides.

Nuclide	Number of samples	MCS ENDF/B-VII.1	
		Average[a]	σ[b]
^{234}U	14	1.051	0.092
^{235}U	14	1.009	0.011
^{236}U	14	0.987	0.019
^{238}U	14	0.999	0.001
^{237}Np	5	0.992	0.017
^{238}Pu	14	1.033	0.070
^{239}Pu	14	1.052	0.037
^{240}Pu	14	1.049	0.028
^{241}Pu	14	1.037	0.046
^{242}Pu	14	1.031	0.040
^{241}Am	14	1.161	0.196
^{243}Am	14	1.031	0.064
^{242}Cm	14	1.039	0.195
^{243}Cm	10	0.941	0.124
^{244}Cm	14	1.060	0.092
^{245}Cm	9	1.187	0.144
^{246}Cm	8	0.825	0.216

[a] Mean of sample (C/E) distribution calculated as $Average = \frac{1}{n}\sum_{i=1}^{n}\left(\frac{C}{E}\right)_i$

[b] Standard deviation of sample (C/E) distribution calculated as $\sigma = \sqrt{\frac{1}{n-1}\sum_{i=1}^{n}\left[\left(\frac{C}{E}\right)_i - Average\right]^2}$, where i is the index of the measured sample and n is the total number of fuel samples measured.

Table 5
C/E results for fission products.

Nuclide	Number of samples	MCS ENDF/B-VII.1	
		Average[1]	σ^2
^{106}Ru	14	1.259	0.252
^{134}Cs	14	0.973	0.029
^{137}Cs	14	0.987	0.017
^{144}Ce	14	1.031	0.059
^{142}Nd	5	0.874	0.057
^{143}Nd	14	0.968	0.014
^{144}Nd	14	0.949	0.031
^{145}Nd	14	0.995	0.014
^{146}Nd	14	0.996	0.023
^{148}Nd	14	1.007	0.016
^{150}Nd	14	1.011	0.017
^{154}Eu	14	1.149	0.055
^{147}Sm	5	1.017	0.011
^{148}Sm	5	0.995	0.015
^{149}Sm	5	0.999	0.052
^{150}Sm	5	1.064	0.008
^{151}Sm	5	0.987	0.023
^{152}Sm	5	1.049	0.006
^{154}Sm	5	1.101	0.009

[1,2] See footnote of Table 4.

Table 6
C/E − 1 results for actinides (%)[a].

Nuclide	MCS ENDF/B-VII.1	MCS ENDF/B-VII.0
^{234}U	4.80	4.73
^{235}U	−0.38	−0.13
^{236}U	−0.15	−0.01
^{238}U	−0.07	−0.07
^{237}Np	−0.70	−0.14
^{238}Pu	−1.43	−11.22
^{239}Pu	2.03	2.83
^{240}Pu	6.48	6.64
^{241}Pu	−0.22	−0.35
^{242}Pu	0.43	−2.98
^{241}Am	−4.26	6.66
^{243}Am	−4.40	7.02
^{242}Cm	29.32	23.41
^{243}Cm	−0.36	−23.76
^{244}Cm	−1.96	−2.30
^{245}Cm	5.94	10.41
^{246}Cm	−14.30	−7.14

[a] Only for SF97-4 sample.

continue the discussion with the analysis of some of the results according to fuel rod type. Then the effect of statistical uncertainties in the Monte Carlo depletion calculation is discussed. Finally, we complete the discussion by comparing MCS depletion results to other depletion codes.

4.1. Discussion of ENDF/B-VII.1 results

As illustrated in Table 4 for the ENDF/B-VII.1 results, the uranium isotopes ^{234,235,236}U are predicted on average by about 5%, 1%, and less than 1.5%, respectively. ^{234}U is overestimated and similar overestimation has also been reported using SCALE (ENDF/B-VII.0) and CASMO (JENDL-4.0) code systems and data libraries [31,32]. Plutonium isotopes ^{238,241,242}Pu are predicted on average within less than 4%. The large underestimation of ^{238}Pu with ENDF/B-VII.0 (10% on average) has been eliminated due to the decrease of the ^{238}Pu(n, γ) and increase of the ^{239}Pu(n, $2n$) one-group cross-sections with ENDF/B-VII.1.^{241}Am is overestimated by about 16% and ^{243}Am is well predicted by 3%, on average. A portion of ^{241}Am is produced by ^{241}Pu (β^- decay). However, ^{241}Pu is overestimated by about 4%. This cannot explain the 16% overestimation of ^{241}Am. ^{241}Am is lost by (n, γ), (n, $2n$) reactions and alpha decay of itself. An underestimation of the ^{241}Am (n, γ) cross section could be partially responsible for the overestimation of ^{241}Am. Curium isotopes ^{242,244}Cm contribute to neutron source in spent fuel for cooling times less than 100 years. ^{243,244,245}Cm are important in burnup credit criticality safety analysis of MOX fuel. On average, the important curium isotopes are predicted within 6%, except for ^{245}Cm. Curium isotopes are largely sensitive to uncertainties in the burnup, considering that they are at the end of the depletion chain.

Table 5 shows that samarium isotopes are predicted on average within 5%, except for ^{150,154}Sm which is overestimated by about 7% and 10%, respectively. ^{149}Sm and ^{151}Sm are very important burnup credit fission product isotopes because of their large neutron capture cross sections. Cesium isotopes are predicted on average within less than 3% of experiment. ^{134}Cs is important in decay heat studies of spent fuel in the first ten years after discharge. ^{137}Cs is important for decay heat at long cooling times over 100 years. One of the fission products which dominates spent fuel decay heat in the first ten years after discharge from reactor, ^{144}Ce, is predicted on average within ~6%. Among the neodymium isotopes, ^{143,145}Nd are important in burnup credit applications and are well predicted on average by 3% and within 1%, respectively. On average, the burnup indicators, ^{145,146,148,150}Nd, show good agreement with experiment, by about 1%. ^{154}Eu is largely overestimated by about 15%. This may be due to an underestimation of the ^{154}Eu (n, γ) cross section.

4.2. Analysis of ENDF/B-VII.1 and ENDF/B-VII.0 result

This section examines the difference in results due to the change of nuclear data library from ENDF/B-VII.0 to ENDF/B-VII.1. Previously, MCS uses ENDF/B-VII.0 data, however, ENDF/B-VII.1 is the data library currently used for production. ENDF/B-VII.0 and ENDF/B-VII.1 results are compared in Tables 6 and 7 for the SF97-4 sample based on the fuel assembly model. The results indicate similar agreement between calculation and experiment for most of the nuclides, with a few exceptions, notably among the actinides:

- ^{238,242}Pu (about 10% and 2.5% difference, respectively, going from ENDF/B-VII.0 to ENDF/B-VII.1);
- ^{241,243}Am (about 2.5% difference, respectively);
- ^{243,245}Cm (about 23% and 5% difference, respectively);

The purpose of the comparison between numerical results of ENDF/B-VII.0 and ENDF/B-VII.1 is to identify the sources of the differences observed in the results. The effect of the library data on the result for the nuclides which show differences is assessed. An investigation of the one-group cross sections tallied by MCS and used in the depletion calculation was carried out to identify which specific data is responsible for the differences in Table 6. ^{238}Pu can be produced by ^{239}Pu (n, $2n$) reaction and destroyed by the ^{238}Pu (n, γ) reaction. As can be seen in Table 6, ^{238}Pu is underestimated by about 11% using ENDF/B-VII.0. Tables 8 and 9 show that the difference in the ^{238}Pu C/E ratio (see Table 6) is due to the decrease of the ^{238}Pu (n, γ) cross-section and increase of the ^{239}Pu (n, $2n$) cross-section from ENDF/B-VII.0 to ENDF/B-VII.1.^{242}Pu is underestimated by about 3% when using ENDF/B-VII.0. A decrease of the ^{242}Pu (n, γ) cross-section in ENDF/B-VII.1 leads to a very good agreement within 0.5%. ^{241}Am is overestimated by about 7% in ENDF/B-VII.0. An increase of the ^{241}Am (n, γ) cross-section in ENDF/B-VII.1 decreases this bias to within 5%. ^{234}Am is overestimated by about 7% with ENDF/B-VII.0. The bias is now within less than 5% due to the increase of the ^{243}Am (n, γ) cross-section. ^{243}Cm shows a large underestimation (about 24%) with ENDF/B-VII.0 which is significantly reduced when using ENDF/B-VII.1, most likely due to

Table 7
C/E − 1 results for fission products (%)[a].

Nuclide	MCS ENDF/B-VII.1	MCS ENDF/B-VII.0
^{106}Ru	16.10	16.59
^{134}Cs	−1.69	0.68
^{137}Cs	−1.74	−1.24
^{144}Ce	12.79	12.77
^{143}Nd	−1.31	−1.18
^{144}Nd	−5.63	−5.70
^{145}Nd	1.07	−0.62
^{146}Nd	0.02	1.36
^{148}Nd	1.82	1.60
^{150}Nd	2.37	1.97
^{154}Eu	8.03	5.31
^{147}Sm	0.34	0.41
^{148}Sm	−1.67	−2.11
^{149}Sm	5.23	5.02
^{150}Sm	6.00	5.59
^{151}Sm	−2.05	−1.82
^{152}Sm	4.31	3.02
^{154}Sm	10.82	10.01

[a] See footnote of Table 6.

Table 8
MCS one-group (n, γ) cross sections (barns).

Nuclide	ENDF/B-VII.1	ENDF/B-VII.0	Difference[a] (%)
^{238}Pu	20.69	29.95	44.75
^{242}Pu	25.96	28.56	10.03
^{241}Am	108.19	94.14	−12.99
^{243}Am	53.41	47.54	−10.99
^{242}Cm	5.09	4.11	−19.16
^{244}Cm	17.25	18.16	5.27

[a] Calculated as $100*\left(\frac{\text{ENDF/B}-\text{VII.0}}{\text{ENDF/B}-\text{VII.1}}-1\right)$.

increase of the ^{242}Cm (n, γ) cross-section. ^{245}Cm is overestimated by about 10% using ENDF/B-VII.0. The overestimation is however reduced to about 6% in ENDF/B-VII.1, thanks to the decrease of the ^{244}Cm (n, γ) cross-section.

4.3. Analysis of results by fuel rod type

Table 10 presents the average (C/E − 1) for the nuclides ^{237}Np, ^{241}Am, ^{245}Cm, ^{106}Ru and ^{154}Eu established separately for each fuel rod, to identify possible bias due to fuel rod location in the assembly. These nuclides show large (C/E − 1) and standard deviation. The uncertainties in number densities of ^{239}Pu in the SF95 and SF97 rod samples could be largely affected by uncertainties in the inter-assembly water gap, because these rods are located on the periphery of the assembly [30].

As can be seen in Table 10, the ^{237}Np (C/E − 1) average is dominated by the SF96 rod samples. This is caused by the large overestimation of ^{237}Np in the samples from the gadolinium bearing rod SF96 (see Table C in the appendix). The overestimation of ^{237}Np in the SF96 samples have also been observed in the analyses of the same PIE data with CASMO calculations based on the JENDL-4.0 library [32]. Without the SF96 samples, ^{237}Np is well predicted on average within 1% (see Table 4). The ^{237}Np results from the SF96 samples are not included in Table 4.

For ^{241}Am, the (C/E − 1) trend shows strong overestimations in the SF95 and SF96 rod fuel samples. ^{241}Am is overestimated on average in the SF97 samples by about 4%. At the time of measurement, the PIE data for all nuclides from the Takahama-3 experiment were corrected back to the date of reactor discharge, except for samarium isotopes [10]. The amount of ^{241}Am during measurement

Table 9
MCS one-group (n, $2n$) cross sections (barns).

Nuclide	ENDF/B-VII.1	ENDF/B-VII.0	Difference[a] (%)
^{239}Pu	1.37E-03	1.34E-03	−2.42
^{241}Am	4.27E-04	4.13E-04	−3.35

[a] See footnote of Table 8.

Table 10
C/E − 1 results by fuel rod (%).

Rod	SF95		SF97		SF96	
Nuclide	Average[a]	σ[b]	Average	σ	Average	σ
^{239}Pu	9.74	1.84	2.59	1.69	2.91	0.74
^{237}Np	-[c]	–	−0.77	1.72	48.11	6.08
^{241}Am	15.32	20.67	3.76	9.09	32.49	15.65
^{245}Cm	32.42	9.76	7.72	4.95	–	–
^{106}Ru	25.26	10.89	21.68	37.34	32.13	16.42
^{154}Eu	18.07	3.69	9.08	1.67	18.34	4.16

[a, b] Calculated according to number of samples in each rod.
[c] No data for this rod.

is mostly driven by ^{241}Pu decay. It is noted that large uncertainties had been introduced when the measured ^{241}Am is corrected for the ^{241}Pu contribution. These uncertainties were not accounted for totally and have been underestimated to a large extent by the measurement laboratory [33].

The average (C/E − 1) of ^{245}Cm is largely driven by the SF95 rod samples. ^{245}Cm is not measured in the SF96 rod. ^{245}Cm overestimation is about 8% in the SF97 rod, relatively very low, compared to SF95. For ^{106}Ru, the overestimation in the (C/E − 1) average is consistently observed in the three fuel rods with very large standard deviations. It is challenging to measure ^{106}Ru in spent fuel due to difficulty in dissolving the metallic fission product. ^{154}Eu is also overestimated in all the samples and the average (C/E − 1) is influenced by the fuel samples from the three rods. We also note in Table 10 that the samples have large (C/E − 1) standard deviation (except ^{154}Eu). This could be an indication that the measurement uncertainties of these nuclides are larger than the values reported and/or experimental methods with higher accuracy may be needed. The large standard deviations observed in Tables 4 and 5 are consistent with the reports of other PIE analysis [31,32].

4.4. Effect of statistical uncertainties

In MC depletion calculations, uncertainty in the nuclear data are propagated through the reaction rates and the nuclide number densities. In addition, MC calculation results include statistical uncertainties. The effect of these uncertainties on nuclide number densities needs to be assessed. The aim of this section is to examine the effect of the statistical uncertainties during depletion calculation in MCS. The propagation of uncertainties due to covariance of nuclear data during depletion will be discussed in another report. The propagation of statistical uncertainties during MC depletion calculations have been studied and the number densities uncertainties at the end of depletion have been shown to be small [34,35]. In the MCS code, the statistical uncertainty of number densities from depletion simulations are not calculated. The statistical uncertainties of the reaction rates/one-group cross-sections are calculated by MCS, but they are not propagated during the depletion calculations. In order to examine the effect of the statistical uncertainties of the number densities, we performed 30 independent simulations starting with different random number

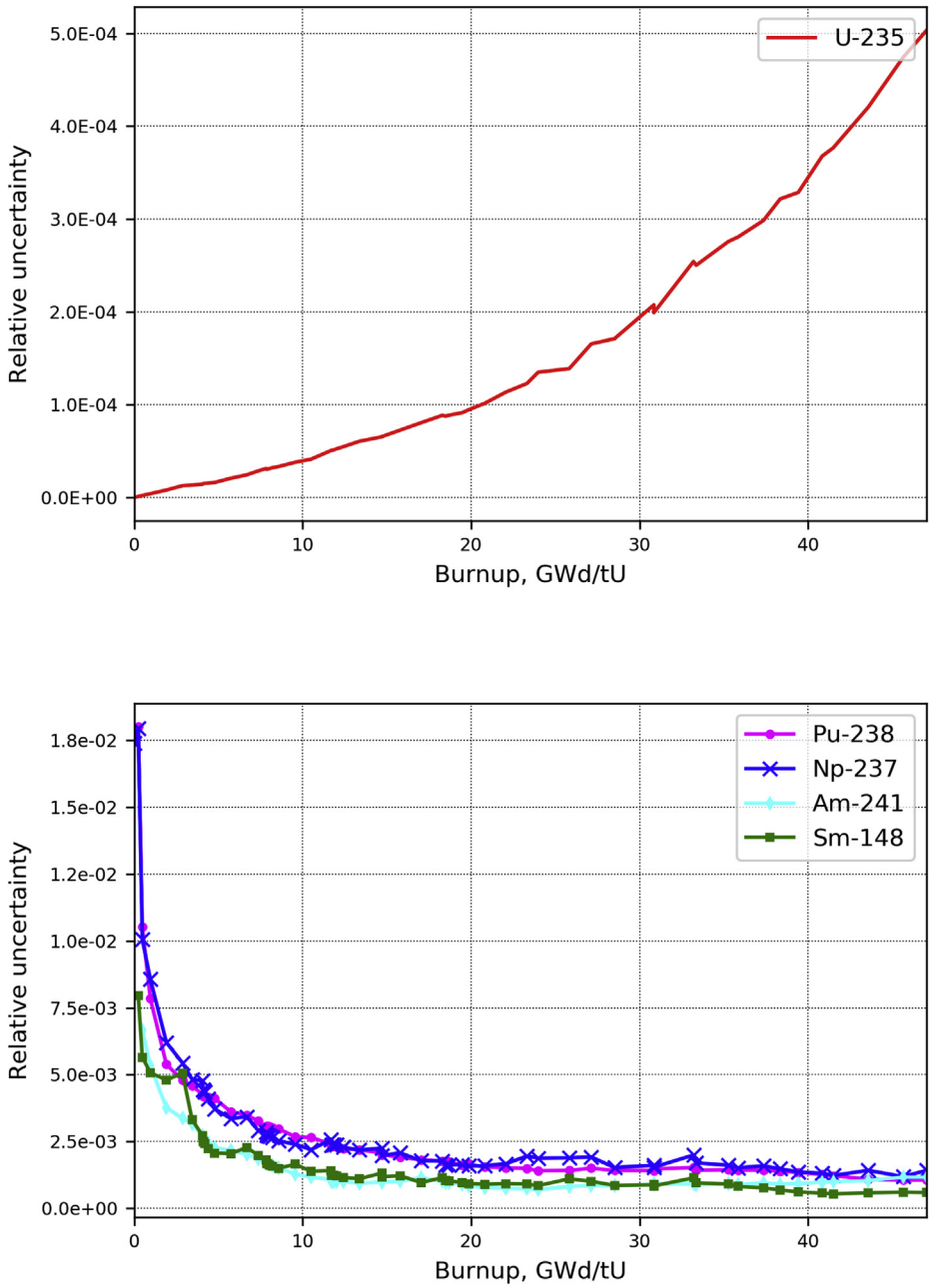

Fig. 2. Statistical uncertainties of nuclide number densities during depletion calculation in MCS.

seeds. The number densities calculated from these multiple simulations are then used to the determine the statistical uncertainties associated with each nuclide number densities at each depletion step. In Fig. 2, we show the relative statistical uncertainty of the nuclide number densities during the depletion calculation for ^{235}U, ^{238}Pu, ^{237}Np, ^{241}Am and ^{148}Sm. These results are obtained from 30 independent pin-cell simulations of the SF97-4 fuel sample (burnup = 47 GWd/tU) with 50 inactive/100 active cycles and 5000 neutron histories. At the beginning of cycle, for all the nuclides analyzed in this work, the maximum statistical uncertainty is less than 1%, except for ^{237}Np, ^{238}Pu, and ^{243}Am. For ^{237}Np, ^{238}Pu, and ^{243}Am, the statistical uncertainties are less than 2% at the beginning of cycle. High uncertainties of ^{237}Np, ^{238}Pu, and ^{243}Am are due to their very small number densities at low burnups. The uncertainties at the end of depletion are less than 0.6% for all the nuclides presented in Tables 4 and 5. At each depletion step, the statistical uncertainties of the capture/fission reaction rates are about 0.2%, and about 2% for the $(n, 2n)$ reaction rate. For all the nuclides presented in Tables 4 and 5, the statistical uncertainties are observed to be small at the end of depletion. The effect of the statistical uncertainties is minimal, even when the number of neutron histories is not large. The statistical uncertainties of the calculated number densities are not included in the evaluation of the $(C/E - 1)$ average and standard deviation.

4.5. Comparison of MCS performance to other depletion codes

The performance of MCS depletion capability is compared to

Table 11
Comparison of C/E − 1 (%) for OECD/NEA BUC benchmark phase 1-B, Case A.

Nuclide	MCS[a]	SCALE[b]	MCNPX[c]	MCNP-ACAB[d]	MONTEBURNS[d]	SERPENT[d]	Experimental uncertainty (%)
^{234}U	−0.9	−0.6	−11.0	−0.1	0.8	−0.9	3.2
^{235}U	−2.7	−4.2	−1.4	−2.6	−2.8	−3.0	3.2
^{236}U	1.4	1.8	1.0	4.1	4.1	1.7	3.2
^{238}U	−0.6	−0.6	−0.6	1.5	1.5	−0.6	3.2
^{238}Pu	−14.5	−13.1	−6.8	−13.3	−10.1	−12.6	3.2
^{239}Pu	−2.1	0.0	−8.5	−0.4	−0.4	−3.0	3.2
^{240}Pu	−3.7	−0.2	−4.8	−0.4	0.4	−1.8	3.2
^{241}Pu	−3.4	−1.8	−2.7	−1.1	−0.9	−1.9	3.2
^{242}Pu	−3.6	−1.6	5.7	1.0	1.0	0.0	3.2
^{133}Cs	−1.0	0.7	−3.0	2.6	2.6	0.1	NA
^{143}Nd	−1.9	0.3	−4.8	2.3	2.1	−0.6	2.0
^{145}Nd	−2.7	−0.7	−4.3	2.1	1.6	−0.8	2.0

NA = not available.
[a] Results from this work.
[b] Results from Ref. [31].
[c] Results from Ref. [1].
[d] Results from Ref. [37].

other depletion codes in this section. The results from the other depletion codes used in this section are based on publicly available information in literature. We did not run these other depletion codes.

4.5.1. Comparison with SCALE and other MC based depletion codes

A comparison of depletion results between MCS, SCALE 6.1, MCNPX, MCNP-ACAB, MONTEBURNS and SERPENT is performed. For this comparison, one PWR fuel sample which is designated as Case A in the OECD/NEA burnup credit (BUC) computational benchmark is analyzed by MCS. The benchmark is a pin cell problem depleted to 27.35 GWd/t burnup. Details of the benchmark problem can be found in the reference [36]. Table 11 shows the comparison of the (C/E − 1) values obtained with MCS, SCALE 6.1, MCNPX, MCNP-ACAB, MONTEBURNS and SERPENT, and the reported experimental uncertainty at two standard deviations. The SCALE depletion sequence used in the calculation is TRITON with the 238-group cross-section library as reported in Ref. [31]. MCNPX results were obtained with MCNP coupled to CINDER90 depletion code [1]. The results from MCNP-ACAB, MONTEBURNS and SERPENT were obtained from the reference [37]. The calculation results of this section are based on the ENDF/B-VII.0 library.

Table 11 shows that the isotopes of plutonium are predicted within the experimental uncertainty by all the codes except for ^{238}Pu which is largely underestimated. Although, MCS predicts ^{240,241,242}Pu slightly outside the experimental uncertainty. ^{235}U is also underestimated by all the codes. ^{234}U is calculated within the experimental uncertainty by all the codes, except for MCNPX. ^{236}U is calculated within the experimental uncertainty by MCS, SCALE 6.1, MCNPX and SERPENT; MCNP-ACAB and MONTEBURNS overestimates ^{236}U by about 4%. ^{133}Cs is predicted within 1% by MCS, SCALE 6.1 and SERPENT, and within 3% by MCNPX, MCNP-ACAB and MONTEBURNS. ^{143}Nd is predicted within the experimental uncertainty by MCS, SCALE 6.1 and SERPENT. Whereas MCS, MCNPX, and MCNP-ACAB predicts ^{145}Nd outside the experimental uncertainty. In general, the code/code comparison showed the performance of MCS relative to other codes. For the presented comparison, MCS performs with reasonably good accuracy compared with other widely used depletion codes.

5. Conclusions

The experimental validation of the Monte Carlo code MCS for SNF applications has been presented. The purpose of the validation is to assess the accuracy and performance of MCS in predicting PWR SNF isotopic compositions. The targeted SNF applications include burnup credit criticality safety analyses, radiation safety, radioactive waste management, decay heat and radiation source terms. The validation range covers 2.6 to 4.1 wt% ^{235}U enrichment and burnup up to 47 GWd/MTU. UO_2 and UO_2-Gd_2O_3 fuels are analyzed. The depletion calculation employs a 2D fuel assembly model, using continuous energy cross section data obtained from ENDF/B-VII.1. The analysis shows average (C/E − 1) within 6% for the actinides ^{234,235,236}U, ^{237}Np, ^{238,239,240,241,242}Pu, ^{243}Am, ^{242,243,244}Cm, and the fission products ^{134,137}Cs, ^{143,145,146,150}Nd, and ^{147,148,149,151,152}Sm. Overall, the validation shows good agreement with measurement for fuel inventory calculations. Moreover, the statistical uncertainties of the nuclide number densities are observed to be small at the end of depletion.

MCS results were also compared to those of other depletion codes using publicly available validation results from literature [1,31,37]. The comparison shows that MCS can predict SNF compositions with accuracy comparable to other code systems. The results presented in this work demonstrate the MCS code as an accurate tool for SNF isotopic inventory prediction.

In the future, the MCS depletion validation work will be expanded to cases of higher enrichment and burnup. The validation of the radiation source term analysis capability of MCS and the propagation of nuclide number density uncertainties during depletion is also planned.

Declaration of competing interest

The authors declare that they have no known competing financial interests or personal relationships that could have appeared to influence the work reported in this paper.

Acknowledgments

This research was supported by the project(L18S015000) by Korea Hydro & Nuclear Power Co. Ltd..

Appendix A

Table A
MCS C/E for Takahama-3 SF95 fuel rod samples.

Sample ID	SF95-1	SF95-2	SF95-3	SF95-4	SF95-5
Burnup (GWd/t)	14.30	24.35	35.42	36.69	30.40
^{234}U	1.091	0.978	1.243	1.236	0.909
^{235}U	1.004	1.017	1.015	1.024	1.008
^{236}U	1.010	0.989	1.005	1.002	0.992
^{238}U	0.999	0.998	0.998	0.998	0.998
^{238}Pu	1.149	1.032	1.151	1.137	1.115
^{239}Pu	1.134	1.089	1.095	1.084	1.086
^{240}Pu	1.070	1.034	1.063	1.073	1.061
^{241}Pu	1.167	1.057	1.064	1.054	1.073
^{242}Pu	1.164	1.034	1.026	1.026	1.059
^{241}Am	0.896	1.153	1.112	1.528	1.077
^{243}Am	1.181	1.077	1.089	1.084	1.098
^{242}Cm	1.103	0.908	0.797	0.682	1.046
^{243}Cm	0.605	0.920	1.097	1.027	0.938
^{244}Cm	1.235	1.069	1.189	1.139	1.218
^{245}Cm	No data	1.173	1.433	1.311	1.381
^{246}Cm	No data	No data	0.932	0.888	1.138
^{106}Ru	1.083	1.268	1.363	1.367	1.183
^{134}Cs	1.014	0.982	1.008	0.992	0.994
^{137}Cs	0.982	0.972	0.981	0.975	0.986
^{144}Ce	0.998	1.000	0.974	1.063	1.007
^{142}Nd	0.783	0.919	0.851	0.868	0.948
^{143}Nd	0.965	0.967	0.967	0.974	0.973
^{144}Nd	0.983	0.973	0.981	0.945	0.978
^{145}Nd	0.999	0.997	0.996	1.000	1.003
^{146}Nd	1.022	1.015	1.017	1.013	1.021
^{148}Nd	1.019	1.014	1.018	1.014	1.019
^{150}Nd	1.009	1.020	1.014	1.013	1.027
^{154}Eu	1.246	1.168	1.177	1.132	1.181

Table B
MCS C/E for Takahama-3 SF97 fuel rod samples.

Sample ID	SF97-2	SF97-3	SF97-4	SF97-5	SF97-6
Burnup (GWd/t)	30.73	42.16	47.03	47.25	40.79
^{234}U	1.088	1.053	1.048	1.048	1.072
^{235}U	0.999	1.001	0.996	0.996	1.005
^{236}U	0.999	1.001	0.998	0.998	0.994
^{238}U	0.999	0.999	0.999	0.999	0.999
^{237}Np	1.006	1.016	0.993	0.993	0.978
^{238}Pu	1.011	1.004	0.986	0.986	1.012
^{239}Pu	1.037	1.035	1.020	1.020	1.042
^{240}Pu	1.063	1.084	1.065	1.065	1.078
^{241}Pu	1.006	1.004	0.998	0.998	1.008
^{242}Pu	1.023	1.010	1.004	1.004	1.009
^{241}Am	1.146	1.075	0.957	0.957	1.104
^{243}Am	0.994	0.974	0.956	0.956	0.996
^{242}Cm	1.185	1.242	1.293	1.293	1.245
^{243}Cm	0.902	0.986	0.996	0.996	0.972
^{244}Cm	1.019	1.008	0.980	0.980	1.031
^{245}Cm	1.066	1.108	1.059	1.059	1.150
^{246}Cm	0.316	0.816	0.857	0.857	0.833
^{106}Ru	1.010	1.052	1.161	1.946	0.913
^{134}Cs	0.907	0.949	0.983	0.979	0.961
^{137}Cs	0.973	0.973	0.983	0.980	0.972
^{144}Ce	0.940	1.038	1.128	1.147	1.018
^{143}Nd	0.984	0.983	0.987	0.978	0.983
^{144}Nd	0.990	0.956	0.944	0.937	0.954
^{145}Nd	1.008	1.006	1.011	1.010	1.005
^{146}Nd	1.004	1.000	1.000	0.999	1.001
^{148}Nd	1.018	1.017	1.018	1.019	1.018
^{150}Nd	1.025	1.025	1.024	1.025	1.029
^{154}Eu	1.093	1.094	1.080	1.068	1.118
^{147}Sm	1.035	1.017	1.003	1.007	1.023
^{148}Sm	1.014	0.997	0.983	0.973	1.009
^{149}Sm	0.922	0.980	1.052	1.062	0.976
^{150}Sm	1.070	1.065	1.060	1.052	1.074
^{151}Sm	1.002	1.000	0.979	0.944	1.007
^{152}Sm	1.060	1.048	1.043	1.048	1.047
^{154}Sm	1.083	1.106	1.108	1.098	1.107

Table C
MCS C/E for Takahama-3 SF96 fuel rod samples.

Sample ID	SF96-2	SF96-3	SF96-4	SF96-5
Burnup (GWd/t)	16.44	28.20	28.91	24.19
^{234}U	0.992	0.985	0.973	0.988
^{235}U	1.010	1.028	1.016	1.011
^{236}U	0.948	0.960	0.962	0.959
^{238}U	1.000	1.000	1.000	1.000
^{237}Np	1.401	1.557	1.520	1.447
^{238}Pu	0.972	0.965	0.965	0.993
^{239}Pu	1.038	1.032	1.018	1.029
^{240}Pu	1.011	1.006	1.005	1.013
^{241}Pu	1.038	1.021	1.016	1.037
^{242}Pu	1.027	1.001	1.015	1.038
^{241}Am	1.470	1.277	1.090	1.463
^{243}Am	1.028	0.990	0.986	1.039
^{242}Cm	0.939	0.897	0.913	0.944
^{244}Cm	0.994	0.982	0.982	1.043
^{106}Ru	1.453	1.289	1.477	1.066
^{134}Cs	0.923	0.976	0.981	0.977
^{137}Cs	0.997	1.009	1.015	1.026
^{144}Ce	0.966	1.068	1.097	0.997
^{143}Nd	0.946	0.948	0.961	0.941
^{144}Nd	0.939	0.881	0.905	0.919
^{145}Nd	0.971	0.971	0.988	0.968
^{146}Nd	0.962	0.957	0.973	0.959
^{148}Nd	0.980	0.978	0.993	0.980
^{150}Nd	0.984	0.981	0.996	0.987
^{154}Eu	1.219	1.116	1.182	1.217

References

[1] L.M. Fensin, J.S. Hendricks, S. Anghaie, The enhancements and testing for the MCNPX 2.6.0 depletion capability, Nucl. Technol. 170 (2010) 68.

[2] G.G. Davidson, T.M. Pandya, S.R. Johnson, et al., Nuclide depletion capabilities in the SHIFT Monte Carlo code, Ann. Nucl. Energy 114 (2018) 259.

[3] H.J. Shim, B.S. Han, J.S. Jung, H.J. Park, C.H. Kim, McCARD: Monte Carlo code for advanced reactor design and analysis, Nucl. Eng. Technol. 44 (2) (2012) 161.

[4] J. Leppanen, M. Pusa, T. Viitanen, et al., The serpent Monte Carlo code: status, development and applications in 2013, Ann. Nucl. Energy 82 (2015) 142.

[5] K. Okumura, T. Mori, M. Nakagawa, K. Kaneko, Validation of a continuous-energy Monte Carlo code MVP-BURN and its application to analysis of post irradiation experiment, J. Nucl. Sci. Technol. 37 (2) (2000) 128.

[6] D. She, Y. Liu, K. Wang, G. Yu, B. Forget, P.K. Romano, K. Smith, Development of burnup method and capabilities in Monte Carlo code RMC, Ann. Nucl. Energy 51 (2013) 289.

[7] H. Lee, Development of a New Monte Carlo Code for Large-Scale Power Reactor Analysis (PhD thesis), Ulsan National Institute of Science and Technology, Ulsan, 2019.

[8] F. Michel-Sendis, I. Gauld, J.S. Martinez, SFCOMPO-2.0: an OECD NEA database of spent nuclear fuel isotopic assays, reactor design specifications, and operations data, Ann. Nucl. Energy 110 (2017) 779.

[9] SFCOMPO 2.0, Spent Fuel Composition Database, Organization for Economic Cooperation and Development, Nuclear Energy Agency, 2017. http://www.oecd-nea.org/sfcompo.

[10] Y. Nakahara, K. Suyama, J. Inagawa, R. Nagaishi, S. Kurosawa, N. Kohno, M. Onuki, H. Mochizuki, Nuclide composition benchmark data set for verifying burnup codes on spent light water reactor fuels, Nucl. Technol. 137 (2) (2002) 111.

[11] J. Jang, W. Kim, S. Jeong, E. Jeong, J. Park, M. Lemaire, H. Lee, Y. Jo, P. Zhang, D. Lee, Validation of UNIST Monte Carlo code MCS for criticality safety analysis of PWR spent fuel pool and storage cask, Ann. Nucl. Energy 114 (2018) 495.

[12] H. Lee, W. Kim, P. Zhang, A. Khassenov, J. Park, J. Yu, S. Choi, H.W. Lee, D. Lee, Preliminary Simulation Results of BEAVRS Three-Dimensional Cycle 1 Wholecore Depletion by UNIST Monte Carlo Code MCS. M&C2017, 2017. Jeju, Korea, April 16-20.

[13] Lee H, Kong C, Lee DJ. Status of Monte Carlo code development at UNIST. In: Proceedings of the PHYSOR Conference; 2014 Sep 28 – Oct 3; Kyoto: Japan. ([USB]).

[14] Lee H., Kim W., Zhang P., Khassenov A., Jo Y., Lee DJ. Development status of Monte Carlo code at UNIST. In: Proceedings of the Korean Nuclear Society Spring Meeting; 2016 May 11-13; Jeju: Korea. ([USB])

[15] M. Lemaire, H. Lee, B. Ebiwonjumi, C. Kong, W. Kim, Y. Jo, J. Park, D. Lee, Verification of photon transport capability of UNIST Monte Carlo code MCS, Comput. Phys. Commun. 231 (2018) 1.

[16] J. Yu, H. Lee, H. Kim, P. Zhang, D. Lee, Preliminary coupling of the thermal/hydraulic solvers in the Monte Carlo code MCS for practical LWR analysis, Ann. Nucl. Energy 118 (2018) 317.

[17] J. Yu, H. Lee, M. Lemaire, et al., MCS based neutronics/thermal-hydraulics/fuel-

performance coupling with CTF and FRAPCON, Comput. Phys. Commun. (2019), https://doi.org/10.1016/j.cpc.2019.01.001.
[18] M. Lemaire, H. Lee, N. Tak, H.C. Lee, D. Lee, Multi-physics steady-state analysis of OECD/NEA modular high temperature gas-cooled reactor MHTGR-350, J. Nucl. Sci. Technol. 54 (6) (2017) 668.
[19] Vutheam Dos, Hyunsuk Lee, Jiwon Choe, Ho Cheol Shin, Hwan Soo Lee, Deokjung Lee*, Validation of UNIST MCS Monte Carlo Code System for OPR-1000, Transaction of KNS Spring Meeting, Jeju, Korea, 2018. May 16-18.
[20] T.Q. Tran, H. Lee, J. Choe, Y. Jo, S. Choi, H.S. Lee, H.C. Shin, D. Lee, Monte Carlo wholecore depletion analysis of yonggwang unit 3 cycles 1 and 2, 2018, in: 6th International Conference on Nuclear and Renewable Energy Resources, NURER, Jeju, Korea, 2018. Sep. 30 - Oct. 3 (2018).
[21] B. Ebiwonjumi, H. Lee, J. Choe, D. Lee, H.C. Shin, MCS Analysis of Westinghouse 3- Loop PWR Multi-Cycle Operation, Korean Nuclear Society Fall Meeting, Yeosu, Korea, 2018. October 25 – 26.
[22] Tung Dong Cao Nguyen, Hyunsuk Lee, Deokjung Lee, VERA Solutions by UNIST MC Code MCS, KNS Spring Meeting, Jeju, Korea, 2018. May 16-18.
[23] Tung Dong Cao Nguyen, Hyunsuk Lee, Jiwon Choe, Matthieu Lemaire, Deokjung Lee, APR-1400 Whole-Core Depletion Analysis with MCS. M&C2019, 2019. Oregon, USA, August 25-29.
[24] A. Khassenov, Generation of Windowed Multipole Library for On-The-Fly Doppler Broadening in UNIST In-House Monte Carlo Code (master's thesis), Ulsan National Institute of Science and Technology, Ulsan, 2018.
[25] J.A. Wash, et al., On-the-fly Doppler broadening of unresolved resonance region cross sections, Prog. Nucl. Energy 101 (2017) 444.
[26] Hyunsuk Lee, Deokjung Lee*, On-The-Fly Interpolation for Thermal Scattering in MCS, Transaction of KNS Spring Meeting, Jeju, Korea, 2018. May 16-18.
[27] M. Pusa, Rational approximations to the matrix exponential in burnup calculations, Nucl. Sci. Eng. 169 (2) (2011) 155.
[28] D. Lee, J. Rhodes, K. Smith, Quadratic depletion method for gadolinium isotopes in CASMO-5, Nucl. Sci. Eng. 174 (2013) 79.
[29] ASTM, Standard test method for atom percent fission in uranium and plutonium fuel (Neodymium-148 Method), Annu. Book ASTM (Am. Soc. Test. Mater.) Stand. 12 (1995) 91, 02(E321-79).
[30] OECD/NEA, State of the Art Report on Spent Nuclear Fuel Assay Data for Isotopic Validation, Organization for Economic Cooperation and Development, Nuclear Energy Agency, Nuclear Science Committee, Working Party on Nuclear Criticality Safety, 2011. Technical Report NEA/NSC/WPNCS/DOC(2011) 5.
[31] G. Ilas, I.C. Gauld, G. Radulescu, Validation of new depletion capabilities and ENDF/B-VII data libraries in SCALE, Ann. Nucl. Energy 46 (2012) 43.
[32] T. Yamamoto, T. Sakai, D. Iwahashi, Analysis of measured isotopic compositions by CASMO5 coupled with a JENDL-4.0 library for irradiated fuel of light water reactors, J. Nucl. Sci. Technol. 54 (3) (2017) 391.
[33] I.C. Gauld, G. Ilas, G. Radulescu, Uncertainties in Predicted Isotopic Compositions for High Burnup PWR Spent Nuclear Fuel, US Nuclear Regulatory Commission, 2011. Technical Report NUREG/CR-7012.
[34] H.J. Park, D.H. Lee, B.K. Jeon, H.J. Shim, Monte Carlo burnup and its uncertainty propagation analyses for VERA depletion benchmarks by McCARD, Nucl. Eng. Technol. 50 (2018) 1043.
[35] M. Tohjoh, T. Endo, M. Watanabe, A. Yamamoto, Effect of error propagation of nuclide number densities on Monte Carlo burn-up calculations, Ann. Nucl. Energy 33 (2006) 1424.
[36] M.D. DeHart, M.C. Brady, C.V. Parks, OECD/NEA Burnup Credit Calculational Criticality Benchmark Phase I-B Results, Oak Ridge National Laboratory, 1996. Technical Report ORNL/TM-6901.
[37] J.S. Martinez, O. Cabellos, C.J. Diez, F. Gilfillan, A. Barbas, Isotopic prediction calculation methodologies: application to Vandellos-II reactor cycles 7-11, in: CD Proceedings of the International Conference on Mathematics and Computational Methods Applied to Nuclear Science and Engineering M&C 2011, 2011.